Unsteady circular Couette flow of a Bingham plastic with the Augmented Lagrangian Method

Rheologica Acta

ISSN 0035-4511
Volume 49
Combined 11-12

Rheol Acta (2010)
49:1197-1206
DOI 10.1007/s00397-010-0497-y

Springer

Rheol Acta (2010) 49:1197–1206
DOI 10.1007/s00397-010-0497-y

ORIGINAL CONTRIBUTION

Unsteady circular Couette flow of a Bingham plastic with the Augmented Lagrangian Method

Larisa Muravleva · Ekaterina Muravleva · Georgios C. Georgiou · Evan Mitsoulis

Received: 10 May 2010 / Revised: 26 September 2010 / Accepted: 12 October 2010 / Published online: 30 October 2010

Abstract Numerical simulations are undertaken for unsteady flows of an ideal Bingham fluid in a circular Couette viscometer. The main difficulties in such simulations are caused by the non-differentiability of the constitutive equation and the need to determine the position and shape of the yield surface separating the yielded zones from the unyielded ones. In this work, these difficulties are overcome by using a numerical method based on variational inequalities, i.e. the augmented Lagrangian/Uzawa method. The start-up and cessation of circular Couette flows of a Bingham fluid are solved numerically assuming that only one of the cylinders is rotating. An improved theoretical upper bound for the stopping time in the case of cessation is derived. The numerical estimates for the stopping time compare well with the theoretical bounds. Moreover, with the adopted method the evolution of the velocity profiles and the locations of yielded/unyielded surfaces are accurately calculated. In flow cessation, we observe an interesting effect, namely the appearance of a small unyielded region adjoined to the outer cylinder shortly before cessation.

Keywords Viscoplasticity · Bingham plastic · Unsteady flows · Variational inequalities · Circular Couette flow · Uzawa method · Augmented Lagrangian method · Computer modeling · Couette viscometry · Yield surface

Paper presented at Workshop on Viscoplastic Fluids: from Theory to Application, November 1–5, 2009, Limassol, Cyprus.

L. Muravleva
Department of Mechanics and Mathematics,
Lomonosov Moscow State University,
Leninskie gory, 1, 119991, Moscow, Russia
e-mail: lvmurav@gmail.com

E. Muravleva
Institute of Numerical Mathematics, Russian Academy of Sciences, Gubkin Street, 8, 119333, Moscow, Russia
e-mail: catmurav@gmail.com

G. C. Georgiou
Department of Mathematics and Statistics,
University of Cyprus, P.O. Box 20537, 1678, Nicosia, Cyprus
e-mail: georgios@ucy.ac.cy

E. Mitsoulis (✉)
School of Mining Engineering & Metallurgy,
National Technical University of Athens,
Zografou, 157 80, Athens, Greece
e-mail: mitsouli@metal.ntua.gr

Introduction

Viscoplastic materials behave as rigid solids, when the imposed stress is smaller than the yield stress, and flow as fluids otherwise. The flow field is thus divided into unyielded (rigid) and yielded (fluid) zones. Two types of rigid zones are traditionally distinguished: the stagnation (dead) zones, where the medium is at rest, and the plug regions (core), where the medium moves as a rigid body. The surface separating a rigid from a fluid zone is known as a yield surface. The location and shape of the latter must be determined as part of the solution of the flow problem.

Two are the main approaches that have been proposed in the literature in order to overcome the aforementioned mathematical difficulties in solving viscoplastic flows. The first one, known as regularization method, consists of approximating the constitutive

equation by a smoother one (e.g., Papanastasiou 1987). The second one is based on the theory of variational inequalities (Duvaut and Lions 1976) by means of which the problem is reduced to the minimization of a functional and requires the solution of the equivalent saddle-point problem by an Uzawa-like algorithm (Fortin and Glowinski 1983). An excellent review of different regularization models and their implementation is given by Frigaard and Nouar (2005). The recent review by Dean et al. (2007) discusses in detail numerical methods based on the variational inequality approach. Moyers-Gonzalez and Frigaard (2004) carried out numerical solutions of duct flows of viscoplastic fluids using both the regularization technique and the augmented Lagrangian method. They concluded that the latter method is superior for certain classes of problems and more effective in determining critical Bingham numbers and pressure gradients at which the flow stops.

In the present work, we consider the time-dependent circular Couette flow of an ideal Bingham fluid between coaxial cylinders. Safronchik (1959) provided a general expression for the velocity and reduced the problem into a nonlinear integral equation, the solution of which has yet to be found. Comparini and De Angelis (1996) pointed out that in start-up flow in a Couette viscometer initiated by suddenly rotating the inner cylinder, the angular velocity tends to the steady solution at infinite time. In the case of cessation flows, however, it is known that in contrast to Newtonian fluids, Bingham plastics come to rest in a finite time. Glowinski (1984) and Huilgol et al. (2002) have proved that this phenomenon takes place for several cessation flows of viscoplastic materials and provided theoretical upper bounds for the stopping times.

Chatzimina et al. (2005, 2007) calculated numerically the stopping times in cessation of plane Couette, and plane, axisymmetric and annular Poiseuille flows by using the regularized Bingham/Papanastasiou constitutive equation. The numerical stopping times were found to be in very good agreement with the theoretical upper bounds, except in a small regime of low to moderate Bingham numbers; in this regime, very high values of the regularization parameter must be used in order to achieve satisfactory accuracy, which requires very long computational times, especially in time-dependent calculations. In a recent work (Muravleva et al. 2010), we have solved the same cessation flow problems with the augmented Lagrangian/Uzawa method to obtain improved results for the stopping times and to determine more accurately the yielded and unyielded regions. It has been demonstrated in particular that the appearance of an unyielded zone near the wall occurs for any non-zero Bingham number in cessation of Poiseuille flow in round tubes as well as in annuli of small radii ratio.

To our knowledge, the numerical modeling of start-up and cessation of the circular Couette flow of Bingham plastics has not been addressed yet. This task is undertaken in the present work using again the augmented Lagrangian/Uzawa method. We also obtain a new theoretical upper bound for the stopping time, which is sharper than that derived by Huilgol et al. (2002). The numerical stopping times are found to agree well with the new stricter theoretical estimates. Accurate results for the location and evolution of the yield surfaces are also presented.

Problem statement

We consider the flow of an incompressible viscoplastic fluid between two coaxial cylinders with outer radius R (cup) and inner radius κR (bob), where $0 < \kappa < 1$. For the sake of simplicity, the possibility of having the two cylinders rotating is excluded. Therefore, either of the cylinders is fixed and the other suddenly starts (start-up) or stops (cessation) rotating with angular speed Ω. Under the assumptions of axisymmetry, sufficiently long cylinders, zero gravity, and incompressibility, the only non-zero velocity component in cylindrical coordinates $(r,\ \theta,\ z)$ is the azimuthal velocity, which is a function of the radial coordinate, r, and the time t, $u_\theta = u_\theta(r,t)$. The corresponding component of the momentum equation for any fluid becomes

$$\rho \frac{\partial u_\theta}{\partial t} = \frac{1}{r^2}\frac{\partial}{\partial r}\left(r^2 \tau_{r\theta}\right), \tag{1}$$

where ρ is the density. The constitutive relation for a Bingham plastic takes the form:

$$\begin{cases} \dot{\gamma}_{r\theta} = 0, & |\tau_{r\theta}| \le \tau_0 \\ \tau_{r\theta} = \tau_0\, sign(\dot{\gamma}_{r\theta}) + \mu \dot{\gamma}_{r\theta}, & |\tau_{r\theta}| > \tau_0 \end{cases}, \tag{2}$$

where μ is a plastic viscosity, τ_0 is the yield stress that needs to be exceeded in order for the fluid to flow, and $\dot{\gamma}_{r\theta}$ is the only non-zero component of the rate-of-strain tensor:

$$\dot{\gamma}_{r\theta} = r\left|\frac{\partial}{\partial r}\left(\frac{u_\theta}{r}\right)\right|. \tag{3}$$

The problem can be conveniently re-written in terms of the angular velocity ω

$$\omega = \frac{u_\theta}{r}. \tag{4}$$

Moreover, the equations are non-dimensionalized scaling the lengths by the outer radius R, the angular

velocity by Ω, the time by $\rho R^2/\mu$, and the stress by $\mu\Omega$. The resulting dimensionless forms of the θ-momentum and the constitutive equations are:

$$\frac{\partial \omega}{\partial t} = \frac{1}{r^3}\frac{\partial}{\partial r}\left(r^2 \tau_{r\theta}\right), \tag{5}$$

and

$$\begin{cases} \dot{\gamma}_{r\theta} = 0, & |\tau_{r\theta}| \le Bn \\ \tau_{r\theta} = Bn\, sign\left(\dfrac{\partial \omega}{\partial r}\right) + r\dfrac{\partial \omega}{\partial r}, & |\tau_{r\theta}| > Bn \end{cases}, \tag{6}$$

where Bn is the Bingham number given by

$$Bn = \frac{\tau_0}{\mu\Omega} \tag{7}$$

Initial and boundary conditions

In *start-up* circular Couette flows, the fluid is initially at rest. The initial and boundary conditions when the inner cylinder suddenly starts rotating are as follows:

$$\omega(r, 0) = 0, \quad \kappa \le r \le 1. \tag{8a}$$

$$\omega(\kappa, t) = 1, \quad \omega(1, t) = 0, \quad t > 0. \tag{8b}$$

In the case where the outer cylinder is rotating we have:

$$\omega(r, 0) = 0, \quad \kappa \le r \le 1. \tag{9a}$$

$$\omega(\kappa, t) = 0, \quad \omega(1, t) = 1, \quad t > 0. \tag{9b}$$

In cessation flows, the angular velocity at $t = 0$ is given by the corresponding steady-state solution ω^s. The initial and boundary conditions read:

$$\omega(r, 0) = \omega^s(r), \quad \kappa \le r \le 1, \tag{10a}$$

$$\omega(\kappa, t) = \omega(1, t) = 0, \quad t > 0. \tag{10b}$$

Steady-state solutions

We summarize the steady-state solutions, which were considered more than 80 years ago by Reiner and Riwlin (1927). Since in steady state, $\partial\omega/\partial t = 0$, then from Eq. 5 one gets: $\tau_{r\theta} = C_1/r^2$, where C_1 is the constant of integration. For both flows of interest, the fluid is fully yielded if the Bingham number is below the critical value

$$Bn_{crit} = \frac{2}{\frac{1}{\kappa^2} - 2\ln\frac{1}{\kappa} - 1}. \tag{11}$$

If $Bn > Bn_{crit}$, the fluid is partially yielded in the region $\kappa \le r \le r_0$, where r_0 is the radius of the cylindrical yield surface, which satisfies the following condition:

$$Bn\left(\frac{r_0^2}{\kappa^2} - 2\ln\frac{r_0}{\kappa} - 1\right) = 2. \tag{12}$$

It is obvious that if there is an unyielded region in the flow, this is always adjacent to the outer cylinder, i.e., in the region $r_0 \le r \le 1$. If the inner cylinder is rotating, the unyielded region is a dead zone (no rotation); if the outer cylinder is rotating, the unyielded region is a rigid body-rotation (plug) zone.

Rotation of the inner cylinder

If $Bn > Bn_{crit}$, the fluid is partially yielded and the angular velocity is given by

$$\omega = \begin{cases} \left(1 + Bn\ln\frac{r_0}{\kappa}\right)\left(\frac{1}{r^2} - \frac{1}{r_0^2}\right)\Big/\left(\frac{1}{\kappa^2} - 1\right) - Bn\ln\frac{r_0}{r}, & \kappa \le r \le r_0 \\ 0, & r_0 \le r \le 1 \end{cases}. \tag{13}$$

If $Bn \le Bn_{crit}$,

$$\omega = \left(1 + Bn\ln\frac{1}{\kappa}\right)\left(\frac{1}{r^2} - 1\right)\Big/\left(\frac{1}{\kappa^2} - 1\right) - Bn\ln\frac{1}{r}, \quad \kappa \le r \le 1. \tag{14}$$

More details for this flow can also be found in Chatzimina et al. (2009).

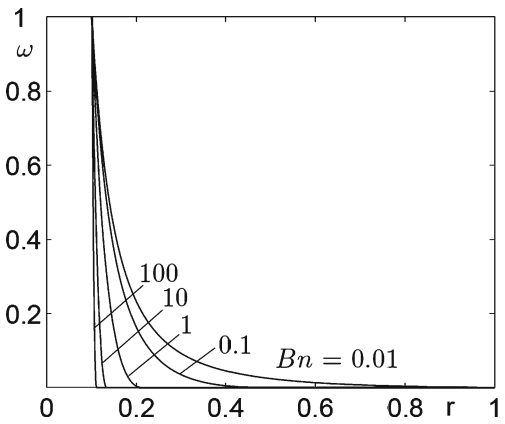

Fig. 1 Steady-state angular velocity profiles for $\kappa = 0.1$ and different Bingham numbers when the inner cylinder is rotating

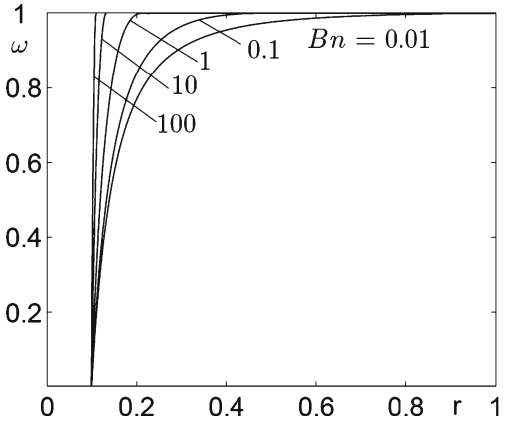

Fig. 2 Steady-state angular velocity profiles for $\kappa = 0.1$ and different Bingham numbers when the outer cylinder is rotating

Rotation of the outer cylinder

If $Bn > Bn_{crit}$,

$$\omega = \begin{cases} \left(1+Bn\ln\frac{r_0}{\kappa}\right)\left(\frac{1}{\kappa^2}-\frac{1}{r^2}\right)\Big/\left(\frac{1}{\kappa^2}-\frac{1}{r_0^2}\right)-Bn\ln\frac{r}{\kappa}, & \kappa\le r\le r_0 \\ 1, & r_0\le r\le 1 \end{cases}. \tag{15}$$

If $Bn \le Bn_{crit}$,

$$\omega=\left(1+Bn\ln\frac{1}{\kappa}\right)\left(\frac{1}{\kappa^2}-\frac{1}{r^2}\right)\Big/\left(\frac{1}{\kappa^2}-1\right)-Bn\ln\frac{r}{\kappa},\ \kappa\le r\le 1. \tag{16}$$

Figures 1 and 2 show steady-state profiles of the annular velocity for the two flows of interest, i.e., for inner- and outer-cylinder rotation, respectively. These were obtained with $\kappa = 0.1$ and different Bingham numbers ranging from 0.01 to 100.

Finite stopping times

The fact that Bingham fluids come to rest in a finite time was proved for plane and axisymmetric Poiseuille and plane Couette flows (Glowinski 1984; Huilgol et al. 2002). The estimates provided are very accurate, and computed stopping times are very close to these bounds either using the regularized Papanastasiou/Bingham model (Chatzimina et al. 2005, 2007) or with the augmented Lagrangian method (Muravleva et al. 2010).

An upper bound for the stopping time, T_f, in the case of circular Couette flow has been reported by Huilgol et al. (2002). In terms of our dimensionless entities, this can be written as follows:

$$T_f = \frac{1}{\lambda_H}\ln\left(1+\frac{\|\omega(0)\|\,\lambda_H}{\beta\,Bn}\right), \tag{17}$$

where $||\omega(t)||$ is a norm of the $\omega(r, t)$ defined as

$$\|\omega\| = \left(\int_\kappa^1 \omega^2 r^3 \mathrm{d}r\right)^{1/2}, \tag{18}$$

the constant β is given by

$$\beta = \min_{\omega\neq 0}\frac{\int_\kappa^1 r^2\left|\frac{\partial\omega}{\partial r}\right|\mathrm{d}r}{\|\omega\|}, \tag{19}$$

and λ_H is the least positive eigenvalue of the problem

$$\begin{cases} \dfrac{d^2u}{dx^2}+\lambda u = 0 \\ u(-\alpha)=u(\alpha)=0 \end{cases}, \tag{20}$$

where $\alpha = (1-\kappa)/(1+\kappa)$. It turns out that (Huilgol et al. 2002)

$$\lambda_H = \frac{\pi^2\kappa^3}{(1-\kappa)^2}. \tag{21}$$

In the present work we have improved on the upper bound for the stopping time. A new stricter bound is given by

$$T_f = \frac{1}{\lambda_1}\ln\left(1+\frac{\|\omega(0)\|\lambda_1}{\beta\,Bn}\right), \tag{22}$$

where λ_1 is the smallest (positive) eigenvalue of the problem:

$$\begin{cases} \dfrac{d^2u}{dr^2}+\dfrac{1}{r}\dfrac{du}{dr}-\dfrac{1}{r^2}u+\lambda u = 0 \\ u(\kappa)=u(1)=0 \end{cases}, \tag{23}$$

Problem (23) is the one that actually corresponds to the Couette flow problem under study; problem (20) is only an approximation valid for small gaps, i.e., for values of κ close to unity. It turns out that λ_1 is the smallest root of

$$Z_1(\lambda) = J_1\left(\kappa\sqrt{\lambda}\right)Y_1\left(\sqrt{\lambda}\right)-J_1\left(\sqrt{\lambda}\right)Y_1\left(\kappa\sqrt{\lambda}\right), \tag{24}$$

where J_1 and Y_1 are the first-order Bessel functions of the first and second kind, respectively.

Another improvement in the present work is the calculation of a stricter upper bound for the constant β defined by Eq. 19. Huilgol et al. (2002) calculated the right-hand side of Eq. 19 for

$$\omega = \alpha^2 - x^2, \qquad -\alpha \le x \le \alpha, \tag{25}$$

and obtained

$$\beta = \frac{(2+\alpha^2)\sqrt{105}}{4\sqrt{7\alpha+3\alpha^3}}. \tag{26}$$

In the present work, however, we used the following function

$$\omega = \left(\alpha^2 - x^2\right)^{1/n}, \qquad -\alpha \le x \le \alpha, \tag{27}$$

where n is an integer. It turns out that

$$\beta(n) = \frac{2\left(1+\frac{n\alpha^2}{n+1}\right)}{\sqrt{\alpha B\left(\frac{1}{2},\frac{2}{n}+1\right)\left(1+\frac{3n\alpha^2}{3n+4}\right)}}, \tag{28}$$

where

$$B(x,y) = \frac{\Gamma(x)\Gamma(y)}{\Gamma(x+y)}, \tag{29}$$

with Γ being the gamma function. By taking the limit as $n \to \infty$, we get

$$\beta = \sqrt{\frac{2(1+\alpha^2)}{\alpha}} = 2\sqrt{\frac{1+\kappa^2}{1-\kappa^2}}, \tag{30}$$

which is a stricter upper bound for β than Eq. 26.

Results and discussion

A detailed description of the Augmented Lagrangian Method with an Uzawa-like iteration for time-dependent, one-dimensional problems can be found in our recent paper (Muravleva et al. 2010). For the discretization of the one-dimensional domain, we use centered finite differences in space and the fully implicit backward Euler scheme in time. This method is very convenient and easily applicable. Besides the angular velocity and stress distribution calculated at every time step, the radius of the yield surface is also readily available. The results for start-up and cessation Couette flows are presented and discussed below.

Start-up flows

We consider the start-up Couette flow of a Bingham plastic initially at rest, assuming that one of the two cylinders suddenly starts rotating. For most of the results we have chosen $\kappa = 0.1$. According to Eq. 11, the critical Bingham number, below which the fluid is fully-yielded in steady state, is $Bn_{crit} = 0.0212$.

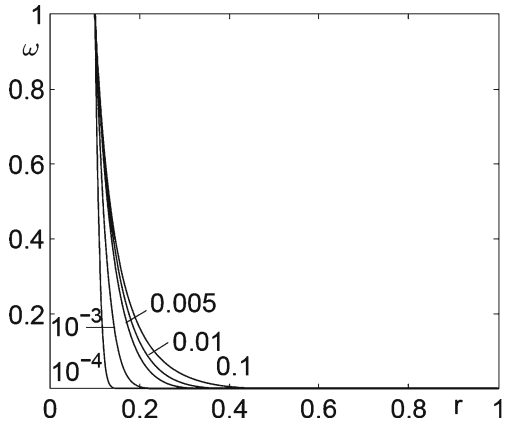

Fig. 3 Evolution of the angular velocity in start-up of Couette flow for $\kappa = 0.1$ and $Bn = 0.1$ when the inner cylinder is rotating

Rotation of the inner cylinder

The evolution of the angular velocity for $Bn = 0.1$, i.e., a value above Bn_{crit}, is shown in Fig. 3. Initially, the angular velocity is nonzero only near the rotating cylinder, and most of the material remains at rest. The yielded region develops very quickly, reaching eventually the steady-state yield surface. Figure 4 shows the evolution of the yield radius, $r_0(t)$, for different values of the Bingham number, i.e., $Bn = 0.02$, 0.05, and 0.1. For $Bn = 0.05$ and 0.1, that is for values above the critical Bingham number, the yield surface moves from the inner cylinder reaching the steady-state radius, r_0. For $Bn = 0.02$, the yield-surface reaches the outer cylinder, since in this case the steady-state solution is fully yielded. It should also be noted that as Bn increases the steady-state solution is reached faster.

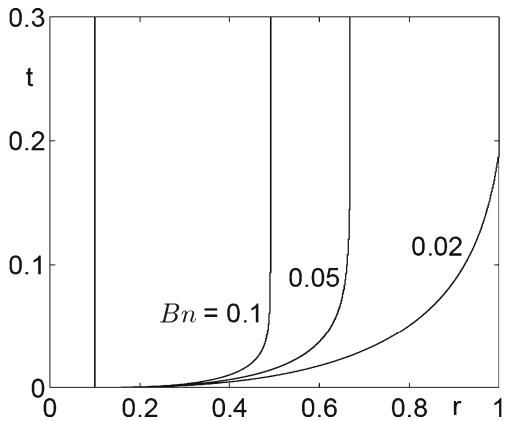

Fig. 4 Evolution of the yield surface in start-up of Couette flow for $\kappa = 0.1$ and different Bingham numbers when the inner cylinder is rotating

Rotation of the outer cylinder

The evolution of the angular velocity for $Bn = 0.1$ is depicted in Fig. 5. The yielded region appears near the rotating outer cylinder and moves quickly towards the fixed inner cylinder. Simultaneously with the start of the motion, a plug region is formed in the middle of the gap. Hence, three moving layers are formed between the cylinders (in the sequence fluid–solid–fluid). In Fig. 5 we can clearly observe flat sections of the velocity profiles at times $t = 0.015$ and 0.03. The velocity increases everywhere in the gap approaching the steady-state solution, which for $Bn = 0.1$ ($> Bn_{crit}$) involves a plug region. The latter, once it is formed, increases in size reaching the steady-state yield surface.

In Fig. 6, we turn our attention to the evolution of the yield surface. At start-up, the rigid zone fills the whole area (the material is at rest), but after the outer cylinder starts rotating, this zone is diminishing and disappears quickly. We observe a plug region inside the gap, which disappears in a short time, after which all the material is yielded. Later on, a new rigid zone adjacent to the rotating outer cylinder appears, which develops to reach the steady-state solution.

To investigate the effect of the yield stress for different Bingham numbers, we show in Fig. 7 the evolution of the yield surface for $Bn = 0.01, 0.05, 0.1$. An initial plug region appears near the inner cylinder. The detailed evolution of the initial rigid zone for these cases is presented on the inset. For the smaller values of Bn, the rigid zone disappears faster. Later, a plug zone arises near the outer cylinder, provided that the Bingham number exceeds the critical value, i.e., for $Bn = 0.1$ and 0.05, but not for $Bn = 0.01$.

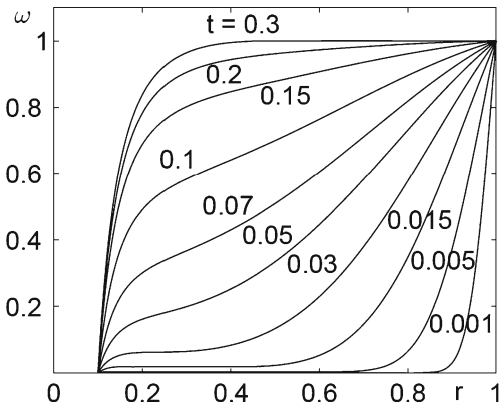

Fig. 5 Evolution of the angular velocity in start-up of Couette flow for $\kappa = 0.1$ and $Bn = 0.1$ when the outer cylinder is rotating

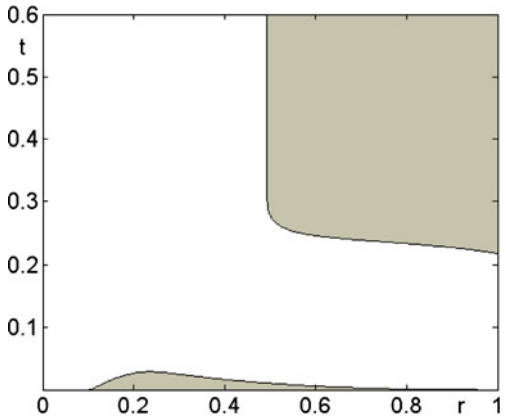

Fig. 6 Evolution of the yield surface in start-up of Couette flow for $\kappa = 0.1$ and $Bn = 0.1$ when the outer cylinder is rotating; the *shaded areas* are unyielded

Cessation flows

We now consider time-dependent flows of a Bingham plastic in the Couette geometry starting from a steady-state solution and assuming that the moving cylinder stops rotating at $t = 0$.

Rotation of the inner cylinder

The evolution of the angular velocity in cessation of the steady flow for $Bn = 0.1$ and $\kappa = 0.1$, when the inner cylinder stops rotating, is shown in Fig. 8. The velocity diminishes very quickly only in the narrow layer adjoined to the bob. Later on, the velocity profiles are gradually decreased in the whole domain. At steady state, there is no plug region, while during cessation we observe a small plug region, which is characterized by a flat angular velocity profile.

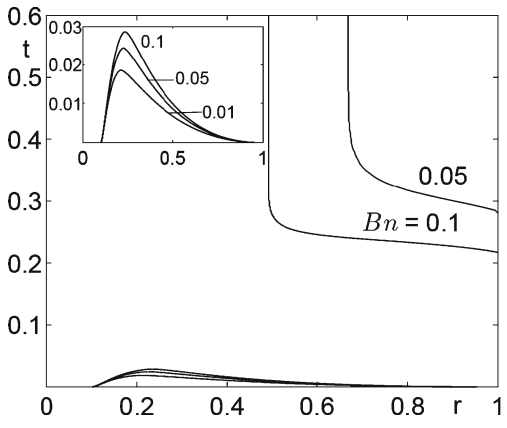

Fig. 7 Evolution of the yield surface in start-up of Couette flow for $\kappa = 0.1$ and different Bingham numbers when the outer cylinder is rotating

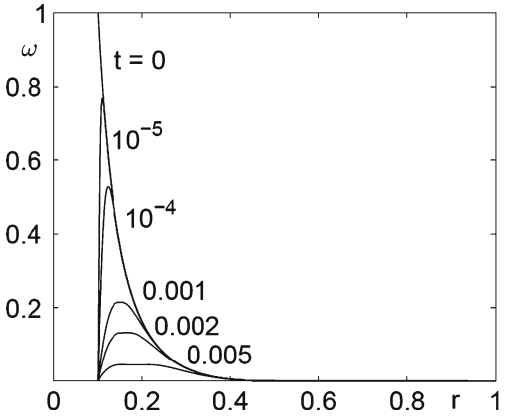

Fig. 8 Evolution of the angular velocity in cessation of Couette flow for $\kappa = 0.1$ and $Bn = 0.1$ when the inner cylinder suddenly stops rotating

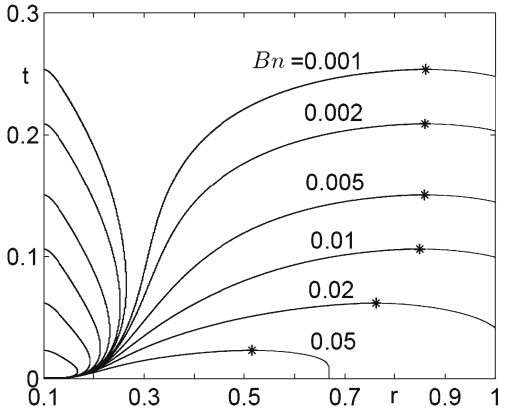

Fig. 10 Evolution of the yield surface in cessation of Couette flow for $\kappa = 0.1$ and different Bingham numbers when the inner cylinder suddenly stops rotating. The *stars* denote the points where the rigid zones meet the dead zones adjacent to the inner cylinder

The evolution of the yield surfaces in Fig. 9 is more impressive. There are two distinct regions at steady state: a dead zone adjacent to the outer cylinder and a yielded region adjacent to the inner cylinder. Initially, the plug region appears and increases in size, while the dead zone does not change. Then, the size of the dead zone increases and the material adheres to the outer cylinder. Hence, the dead zone and the plug region approach and eventually join each other. The star on this and subsequent figures designates the point at which the plug region and the zero-velocity region meet.

The analogous effect, i.e. the existence of a second unyielded region of a smaller size appearing near a fixed wall, was first noted by Chatzimina et al. (2005) in circular Poiseuille flow for a certain value of the Bingham number. In our recent paper (Muravleva et al. 2010), we have shown that this effect takes place for all Bingham numbers. Moreover, the same behavior can be observed in annular Poiseuille flow for small values of the diameter ratio. The appearance of a dead region near the outer cylinder (wall static layer) is an inherent feature of the solution. The evolution of the yield surfaces for $\kappa = 0.1$ and different Bingham numbers is depicted in Fig. 10. Similar results for $\kappa = 0.5$ are shown in Fig. 11. One may observe that the size of the wall static layer increases with the Bingham number. It should be noted that for $\kappa = 0.9$, no dead zones have been observed.

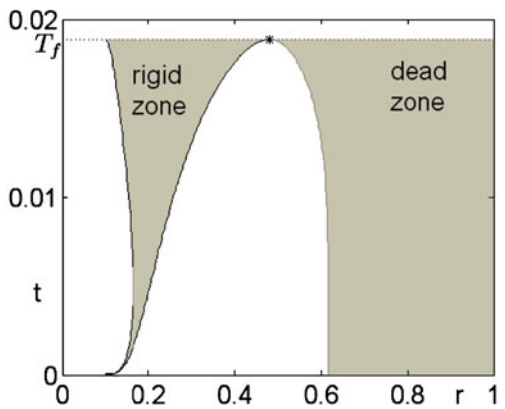

Fig. 9 Evolution of the yield surface in cessation of Couette flow for $\kappa = 0.1$ and $Bn = 0.1$ when the inner cylinder suddenly stops rotating. The *shaded regions* are unyielded. The *star* denotes the point where the rigid zone meets the dead zone adjacent to the inner cylinder. T_f is the upper bound for the stopping time given by Eq. 22

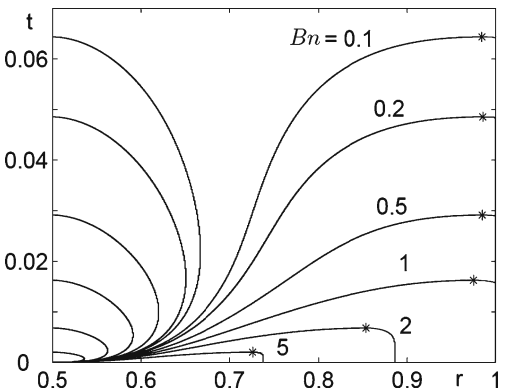

Fig. 11 Evolution of the yield surface in cessation of Couette flow for $\kappa = 0.5$ and different Bingham numbers when the inner cylinder suddenly stops rotating. The *stars* denote the points where the rigid zones meet the dead zones adjacent to the inner cylinder

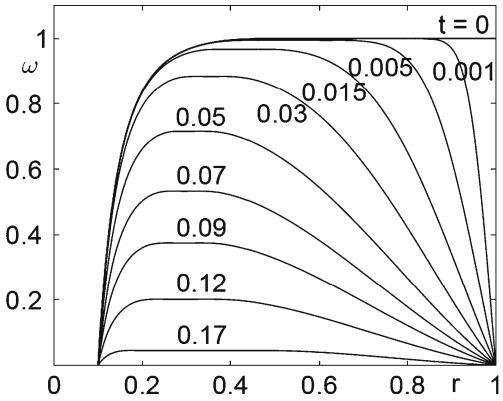

Fig. 12 Evolution of the angular velocity in cessation of Couette flow for $\kappa = 0.1$ and $Bn = 0.1$ when the outer cylinder suddenly stops rotating

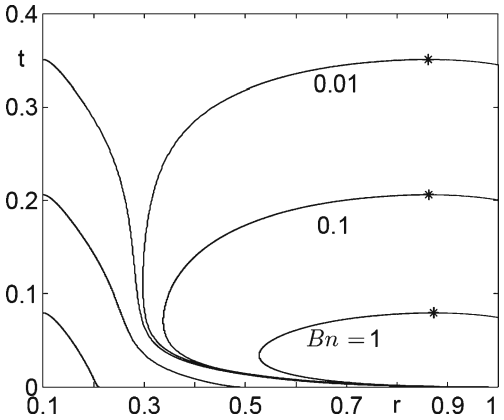

Fig. 14 Evolution of the yield surface in cessation of Couette flow for $\kappa = 0.1$ and different Bingham numbers when the outer cylinder suddenly stops rotating. The *stars* denote the points where the rigid zones meet the dead zones adjacent to the inner cylinder

Rotation of the outer cylinder

We now consider the cessation of Couette flow when the outer cylinder stops rotating. Figure 12 shows the evolution of the angular velocity for $Bn = 0.1$. At steady state ($t = 0$), there is a plug region adjacent to the rotating outer cylinder. Initially, the velocity profile near the inner cylinder is essentially unchanged, while the velocity near the outer cylinder decreases very quickly. The plug region becomes smaller and moves towards the inner cylinder. As time progresses, the velocity of the whole ring gap gradually decreases, the plug region continues moving to the left, and the velocity profiles become more asymmetric. Later still, the velocity decreases, and the size of the unyielded region becomes bigger. In addition, at a certain time shortly before cessation, a stagnant zone near the outer cylinder appears and increases rapidly.

The evolution of the yield surface for this flow is depicted in Fig. 13. The size of the plug region is reduced in the beginning of cessation and increases later on. Its right limit initially moves to the left, but at longer times, it starts moving to the right, as the flow approaches complete cessation. The appearance of the dead zone and its growth can be easily seen. The development of the yield surfaces for different Bingham numbers for $\kappa = 0.1$ and 0.5 are depicted in Figs. 14 and 15, respectively. The size of the wall static layer decreases with increasing Bn number (it is hardly visible on the figures as the changes are very small). For $\kappa = 0.5$, the wall static layer is sufficiently less than that for $\kappa = 0.1$.

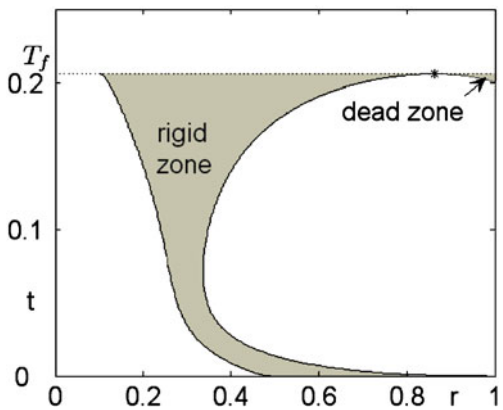

Fig. 13 Evolution of the yield surface in cessation of Couette flow for $\kappa = 0.1$ and $Bn = 0.1$ when the outer cylinder suddenly stops rotating. The *shaded regions* are unyielded. The *star* denotes the point where the rigid zone meets the dead zone adjacent to the inner cylinder. T_f is the upper bound for the stopping time given by Eq. 22

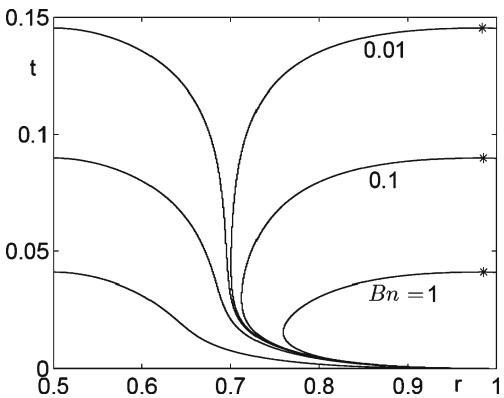

Fig. 15 Evolution of the yield surface in cessation of Couette flow for $\kappa = 0.5$ and different Bingham numbers when the outer cylinder suddenly stops rotating. The *stars* denote the points where the rigid zones meet the dead zones adjacent to the inner cylinder

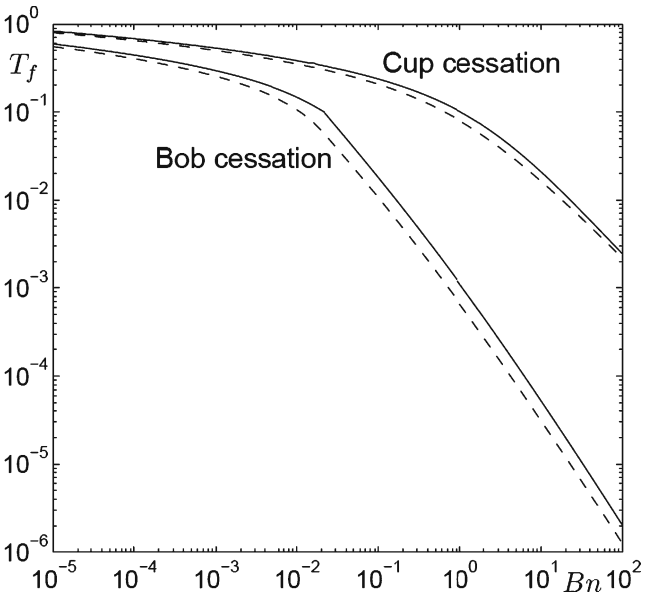

Fig. 16 Comparison of the computed stopping times T_f (*dashed lines*) with the theoretical upper bounds (*solid lines*) for $\kappa = 0.1$

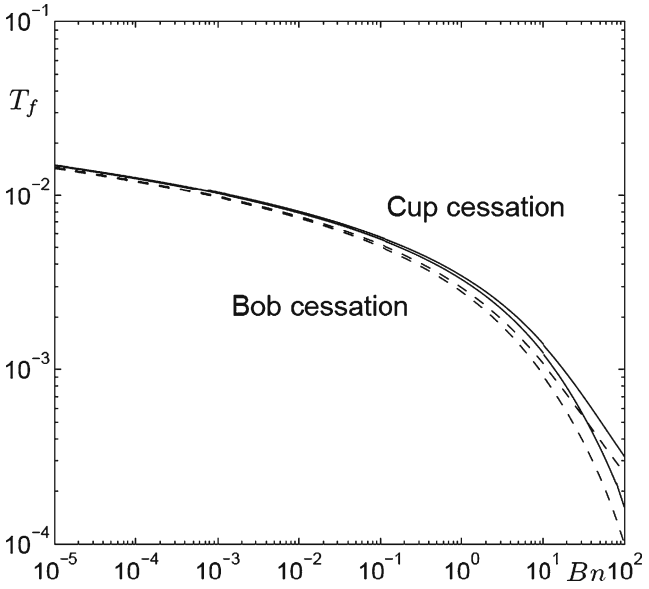

Fig. 18 Comparison of the computed stopping times T_f (*dashed lines*) with the theoretical upper bounds (*solid lines*) for $\kappa = 0.9$

The numerical stopping times for $\kappa = 0.1, 0.5$, and 0.9 are compared with the theoretical upper bounds given by Eq. 22 in Figs. 16, 17, and 18. The numerical results satisfy the theoretical predictions for the whole range of Bingham numbers. The finite stopping times are always slightly below the theoretical upper bounds for the cup cessation problem. In the case of bob cessation, the discrepancies between the numerical stopping time and the theoretical upper bound are still small but slightly bigger than their counterparts for cup cessation. Some explanations are in order here.

The norm of the steady-state velocity for cup rotation is bigger than for bob rotation (with fixed κ and Bn). Moreover, a plug region (where the velocity exceeds a maximum) adjacent to the outer cylinder exists, and it becomes bigger with increasing Bn. In the case of bob rotation, a dead zone with zero velocity adjacent to the cup exists and becomes larger with increasing

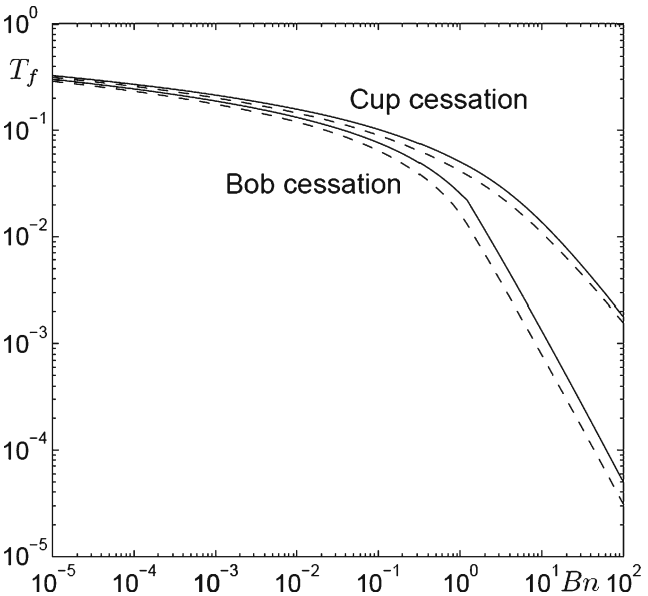

Fig. 17 Comparison of the computed stopping times T_f (*dashed lines*) with the theoretical upper bounds (*solid lines*) for $\kappa = 0.5$

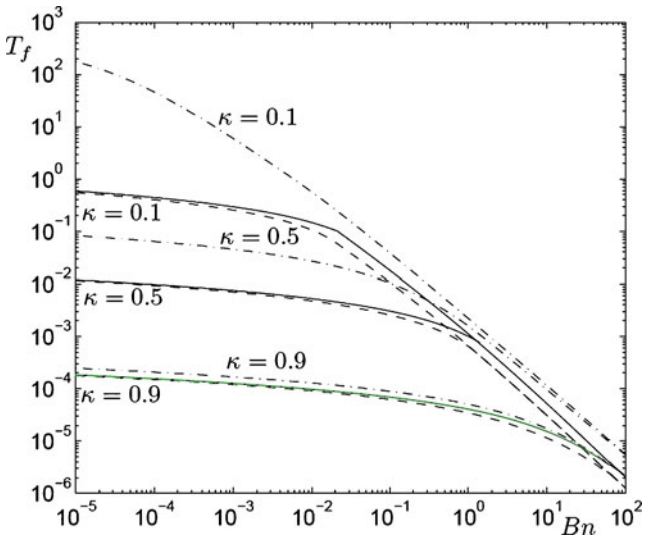

Fig. 19 Comparison of the computed stopping time T_f (*dashed lines*) with the theoretical upper bound (*solid lines*) of Eq. 22 for different Bn numbers ($R_1 = 0.1$, $\kappa = 0.1, 0.5, 0.9$). The *dash–dot–dash lines* are the theoretical upper bounds given by Eq. 17 (Huilgol et al. 2002)

Bn. Therefore, the velocity norm increases with *Bn* for cup rotation and decreases for bob rotation. In Figs. 16, 17, and 18, we see that the theoretical upper bound is tighter for cup cessation than for bob cessation.

The case of cup rotation and of all viscometric flows considered in Muravleva et al. (2010) have no dead zones at steady state. In contrast, at steady state, the case of bob rotation for large values of *Bn* number has a fluid region in $R_1 < r < r_0$ and a dead zone in $r_0 < r < R_2$. Let us fix R_1 and consider several increasing values of R_2. The distribution of the velocity in the fluid region $R_1 < r < r_0$ will be the same, and the dead zone becomes wider. For all the cases where the radius of outer cylinder $R_2 > r_0$ during bob cessation, the angular velocity distribution $\omega(r, t)$ will be the same in the fluid region, and $\omega \equiv 0$ for all $r > r_0(t)$. The stopping times will also coincide for all $R_2 > r_0$. This effect is demonstrated in Fig. 19, where the computed stopping times are compared with the theoretical upper bounds for fixed $R_1 = 0.1$ and three different values of the outer cylinder radius $R_2 = (1/9, 0.2, 1)$ corresponding to $\kappa = (0.9, 0.5, 0.1)$. The small kinks in the theoretical curves do not have any real significance, but they are rather a consequence of not using very small increments in the *Bn* number around this range of continuation.

It would be useful to compare our present results with cessation experiments in Couette flow, but to the best of our knowledge, such data are not available in the open literature for Bingham fluids. Thus, the best we could do was to compare them with the theoretical upper bounds. However, we hope that the present theoretical results can provide an impetus to experimentalists to perform such experiments and do the comparisons with our findings.

Conclusions

The augmented Lagrangian method with an Uzawa-like iteration method is based on variational inequalities and allows accurate calculation of both the evolution of the velocity profiles and the yield surfaces. In the present work, we have solved both start-up and cessation flows of an ideal Bingham plastic in circular Couette geometry, in which only one of the cylinders is rotating while the other is fixed. The appearance, development and elimination of the unyielded regions have been studied extensively. An interesting effect was observed during the cessation of the flow, namely that the dead (unyielded) region adjoined to the outer cylinder appears shortly before flow cessation.

Furthermore, a new theoretical upper bound has been derived for the cessation flow and tested against the numerical solutions. The latter are always lower than the theoretical bounds as they should, and they are much closer in the case of the outer cylinder rotating.

Acknowledgements Financial support from the program "SOCRATES" for scientific exchanges between Greece and Cyprus is gratefully acknowledged. This work was partially supported by the Russian Federation RFBR grant 08-01-00353, 09-01-00565.

References

Chatzimina M, Georgiou GC, Argyropaidas I, Mitsoulis E, Huilgol RR (2005) Cessation of Couette and Poiseuille flows of a Bingham plastic and finite stopping times. J Non-Newton Fluid Mech 129:117–127

Chatzimina M, Xenophontos C, Georgiou G, Argyropaidas I, Mitsoulis E (2007) Cessation of annular Poiseuille flows of Bingham plastics. J Non-Newton Fluid Mech 142:135–142

Chatzimina M, Georgiou G, Alexandrou A (2009) Wall shear rates in circular Couette flow of a Herschel-Bulkley fluid. Appl Rheol 19:34288

Comparini E, De Angelis E (1996) Flow of a Bingham fluid in a concentric cylinder viscometer. Adv Math Sci Appl 6:97–116

Dean EJ, Glowinski R, Guidoboni G (2007) On the numerical simulation of Bingham visco-plastic flow: old and new results. J Non-Newton Fluid Mech 142:36–62

Duvaut G, Lions JL (1976) Inequalities in mechanics and physics. Springer, Berlin

Fortin M, Glowinski R (1983) Augmented Lagrangian Methods: applications to the numerical solution of boundary-value problems. North-Holland, Amsterdam

Frigaard IA, Nouar C (2005) On the usage of viscosity regularization methods for viscoplastic fluid flow computation. J Non-Newton Fluid Mech 127:1–26

Glowinski R (1984) Numerical methods for nonlinear variational problems. Springer, New York

Huilgol RR, Mena B, Piau JM (2002) Finite stopping time problems and rheometry of Bingham fluids. J Non-Newton Fluid Mech 102:97–107

Moyers-Gonzalez MA, Frigaard IA (2004) Numerical solution of duct flows of multiple visco-plastic fluids. J Non-Newton Fluid Mech 122:227–241

Muravleva LV, Muravleva EA, Georgiou GC, Mitsoulis E (2010) Numerical simulations of cessation flows of a Bingham plastic with the Augmented Lagrangian Method. J Non-Newton Fluid Mech 165:544–550

Papanastasiou TC (1987) Flow of materials with yield. J Rheol 31:385–404

Reiner M, Riwlin R (1927) Ueber die Stroemung einer elastischen Flussigkeit im Couette Apparat. Kolloid Z 43:1–5

Safronchik AI (1959) Rotation of a cylinder with variable angular velocity in a visco-plastic medium. J Appl Math Mech 23:1504–1511